PERGAMON

www.elsevier.nl/locate/poly

Polyhedron 19 (2000) 1961–1966

POLYHEDRON

Electronic and NMR properties of *meso*-monosubstituted ferrocenylporphyrin: evidence of π-conjugation between porphyrin and ferrocene

Seog Woo Rhee [b], Byung Bin Park [a], Youngkyu Do [b,*1], Jinkwon Kim[a,*2]

[a] *Department of Chemistry and RRC/NMR, Kongju National University, Kongju 314-701, South Korea*
[b] *Department of Chemistry, School of Molecular Science-BK21 and Center for Molecular Design and Synthesis, Korea Advanced Institute of Science and Technology, Taejon 305-701, South Korea*

Received 29 February 2000; accepted 26 June 2000

Abstract

The reaction of dipyrrylmethane with an equimolar mixture of ferrocenecarboxaldehyde and benzaldehyde in dry acetonitrile in the presence of a catalytic amount of trichloroacetic acid leads to the formation of 5-ferrocenyl-15-phenyl-2,8,12,18-tetraethyl-3,7,13,17-tetramethylporphyrin (**1**) with a yield of 27%. The metallation of **1** with $Zn(OAc)_2 \cdot 2H_2O$ and $MnCl_2 \cdot 4H_2O$ gives Zn·**1** and MnCl·**1**, respectively. Cyclic voltammograms of **1**, Zn·**1** and MnCl·**1** show reversible one-electron oxidation processes for the oxidation of ferrocene at 0.29, 0.22, and 0.37 V, respectively. Variable temperature ^1H NMR spectra of **1** in toluene-d_8 show two distinct singlets of equal intensities and line widths for NH protons. From the plot of ln (k/T) versus $1/T$ according to the Eyring equation, gave straight line with $\Delta G^{\ddagger} = 51$ kJ mol^{-1}. © 2000 Elsevier Science Ltd. All rights reserved.

Keywords: Ferrocenylporphyrin; π-Conjugation; Electrochemical communication; Intramolecular hydrogen bonding; NH tautomerism

1. Introduction

Many discrete molecules in which two photo- and redox-active sites are linked by π-conjugation have been developed with great interest for applications in molecular electronic devices [1,2]. In particular, porphyrins [3,4] or ferrocenes [5] are the most frequently used molecules for this purpose. However, examples of covalently linked π-conjugates of these two units are quite rare [6,7]. These facts and the recent demonstration on the significant substituent effect on electronic properties in porphyrins prompted us to explore new porphyrin–ferrocene conjugates. Herein we describe the synthesis, structure and conjugated feature of 5-ferrocenyl-15-phenyl-2,8,12,18-tetraethyl-3,7,13,17-tetramethylporphyrin (**1**).

2. Experimental

2.1. Materials

Solvents were purified according to standard methods where applicable [8]. Tetra-*n*-butylammonium perchlorate (TBAP) was synthesized and purified by procedure described in the literature [9]. 3,3′-Diethyl-4,4′-dimethyl-2,2′-dipyrrylmethane was synthesized according to procedures described in the literature [10]. All other reagents were purchased from Aldrich Chemical Co. or Sigma Chemical Co. and were used as received.

2.2. Preparations

5-Ferrocenyl-15-phenyl-2,8,12,18-tetraethyl-3,7,13,17-tetramethylporphyrin (**1**) was synthesized by a procedure similar to that described by Osuka et al. for the preparation of 5,15-diarylporphyrins [11]. The ferrocenecarboxaldehyde (0.79 g, 3.7 mmol) and benzaldehyde (0.39 g, 3.7 mmol) were dissolved in dry acetonitrile (84 ml) containing trichloroacetic acid (0.56 g,

---

E-mail address: jkim@knu.kongju.ac.kr (J. Kim).

[1] *Corresponding author

[2] *Corresponding author. Tel.: +82-41-850-8496; fax: +82-41-850-8479

PII: S0277-5387(00)00481-2

3.4 mmol). The mixture was stirred for 30 min under nitrogen. Then, the 3,3′-diethyl-4,4′-dimethyl-2,2′-dipyrrylmethane (1.8 g, 7.4 mmol) in acetonitrile (20 ml) was added through cannula under positive nitrogen pressure. After stirring for 60 h under nitrogen in the dark, *p*-chloranil (2.93 g, 12 mmol) in THF (100 ml) was added and stirred for 5 h under same conditions. The solvent was evaporated to dryness, and the residual solid was suspended on aqueous NaOH solution (10%, 100 ml) to dissolve the hydroquinone impurities. After stirring for 2 h, filtered on a glass frit, washed with water and then methanol. The crude products were separated and purified by flash chromatography (SiO_2, 3.8 × 25 cm, $CHCl_3$). The first red band was 5,15-diphenyl-2,8,12,18-tetraethyl-3,7,13,17-tetramethylporphyrin (**2**), and the second olive green band was the desired 5-ferrocenyl-15-phenyl-2,8,12,18-tetraethyl-3,7,13,17-tetramethylporphyrin (**1**). Recrystallization from toluene–methanol mixture gave purple crystals of **1**·$0.5C_6H_5Me$ (0.70 g, 27% based on the amount used dipyrrylmethane). *Anal.* Calc. for $C_{48}H_{50}N_4Fe{\cdot}0.5C_6H_5Me$ (MW 784.87): C, 78.81; H, 6.93; N, 7.14. Found: C, 77.58; H, 6.93; N, 7.19. ^1H NMR (δ ppm, $CDCl_3$) 9.86 (s, 2H, *meso*-H), 8.25 (d, 1H, phenyl), 7.75 (m, 3H, phenyl), 7.64 (d, 1H, phenyl), 7.25–7.16 (m, 2.5H, phenyl of C_6H_5Me), 4.70 (t, 2H, ferrocenyl), 4.60 (t, 2H, ferrocenyl), 3.90 (m, 8H, CH_2CH_3), 3.72 (s, 5H, ferrocenyl), 3.35 (s, 6H, CH_3), 2.39 (s, 6H, CH_3), 2.35 (s, 1.5H, C_6H_5Me), 1.72 (t, 6H, CH_2CH_3), 1.66 (t, 6H, CH_2CH_3), −1.06 (s, 1H, NH), −1.32 (s, 1H, NH). UV–Vis (C_6H_5Me) [λ_{max}, nm (log ε, $mol^{-1}\ dm^3\ cm^{-1}$)] 421 (5.19), 505 (4.05), 527 (4.01), 581 (3.94), 601 (3.95), 662 (3.53).

Zn·**1** was obtained by treatment of refluxing chloroform solution of **1** with saturated methanolic $Zn(OAc)_2{\cdot}2H_2O$ solution. Recrystallization from chloroform–methanol mixture gave purple crystals of Zn·**1** (77%). MnCl·**1** were obtained by treatment of refluxing chloroform solution of **1** with saturated methanolic $MnCl_2{\cdot}4H_2O$ solution and then by air-oxidation (58%).

Table 1
Details of the crystallographic data collection for **1**·$0.5C_6H_5Me$

Chemical formula	$C_{48}H_{50}N_4Fe{\cdot}0.5C_6H_5Me$
Chemical formula weight	784.87
Space group	*C*2/*c*
a (Å)	50.557(5)
b (Å)	14.611(5)
c (Å)	23.593(3)
β (°)	101.54(2)
V (Å^3)	17076(7)
Z	16
ρ_{calc} (g cm^{-3})	1.255
μ (mm^{-1})	0.395
λ (Mo Kα) (Å)	0.71073
2θ max. (°)	44
Parameters refined	955
$R(F_o)$	0.0780
$wR(F_o^2)$ [a]	0.2032
Goodness-of-fit	1.070

[a] $w = 1/[\sigma^2(F_o^2)+(0.1197P)^2+37.5443P]$ where $P=(F_o^2+2F_c^2)/3$.

2.3. Physical measurements

Elemental analyses (C, H, and N) were performed by Fisons EA 1110 analyzer. ^1H NMR spectra were recorded on a Bruker Spectrospin 400 instrument with chemical shifts being referenced against the signal of the deuterated NMR solvents. Electronic spectra were measured on a Shimadzu UV-3100S spectrophotometer. Thermogravimetric analyses were performed under nitrogen atmosphere at a heating rate of 10°C min^{-1} with DuPont TGA 2050 instrument. Electrochemical measurements were carried out on a BAS-100W system. Cyclic voltammetry was performed with 1×10^{-3} mol dm^{-3} solution of sample in dry CH_2Cl_2 containing 0.1 mol dm^{-3} of $(n\text{-}C_4H_9)_4NClO_4$ as supporting electrolyte. The potentials were determined with reference to the Ag–AgCl electrode at room temperature. Under these conditions ferrocene shows a reversible one-electron oxidation wave ($E_{1/2}=0.37$ V).

2.4. X-ray crystallography

A purple crystal of **1**·0.5 C_6H_5Me with dimensions 0.5 × 0.4 × 0.25 mm, obtained from toluene–methanol solution, was mounted on a thin glass fiber and intensity data were collected on an Enraf–Nonius CAD4 diffractometer equipped with monochromated Mo Kα ($\lambda = 0.71073$ Å) radiation. Unit cell parameters were determined from a least-squares fit of 25 accurately centered reflections ($22.45 < 2\theta < 27.22$). These dimensions and other parameters, including conditions of data collection, are summarized in Table 1. Data were collected at 293 K in the ω–2θ scan mode. Three intense reflections were monitored every 200 reflections to check stability. Of the 9932 unique reflections measured, 6198 were considered observed ($F_o > 4\sigma(F_o)$) and were used in subsequent structure analysis. Data were corrected for Lorentz and polarization effects. Empirical absorption correction using the ψ scan technique was applied. Maximum and minimum transmissions were 99.83 and 96.21%, respectively. The SHELXS-86 program was utilized for the direct method. The structure refinements were performed with the SHELXL-93 program on F^2 data. Anisotropic thermal parameters for all non-hydrogen atoms were included in the refinements. All hydrogen atoms bonded to carbon atoms were included in calculated positions. This C–H bond distance was fixed and U values were assigned based approximately on the U value of the attached atom. The other hydrogens (N–H) were included in located positions with $U = 0.08$ Å^2. The toluene molecule is

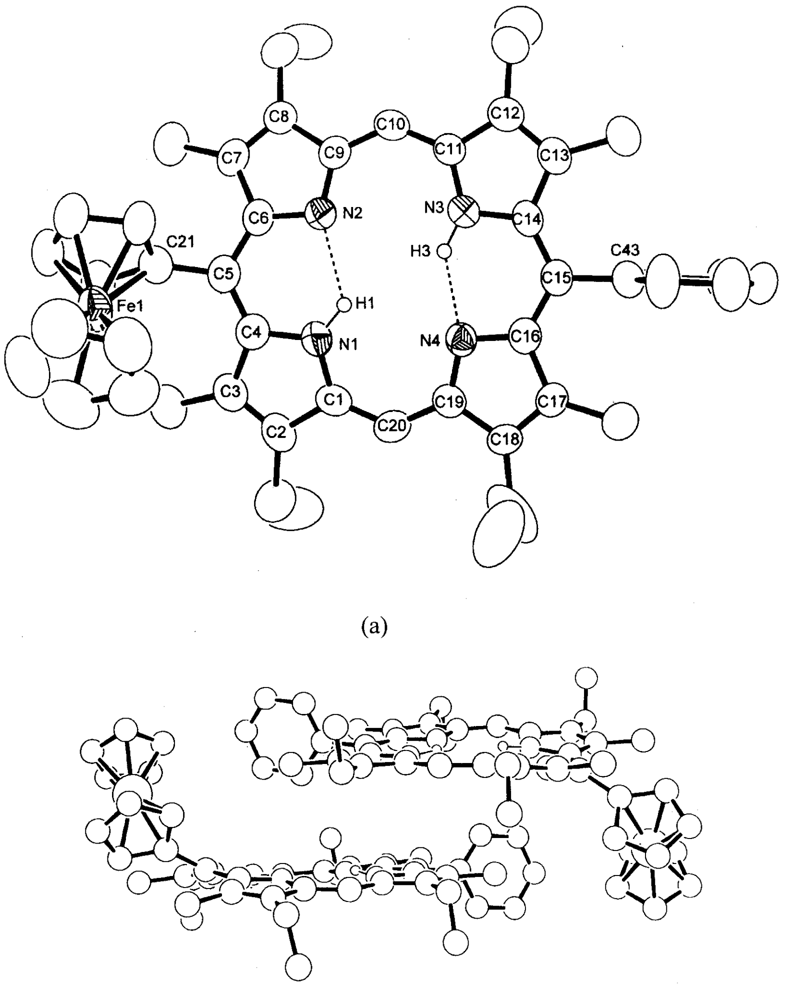

(a)

(b)

Fig. 1. Molecular structure of **1**, monomeric (a), and dimeric (b) structure.

refined with the regular hexagon model ($d_{C–C} = 1.39$ Å). A final difference Fourier map revealed several random features (< 0.627 eÅ^{-3}). The full-matrix least-squares refinement finally converged with $R_1 = 0.0780$ (based on F) and $wR_2 = 0.2032$ (based on F^2) for observed reflections ($F_o > 4\sigma(F_o)$).

3. Results and discussion

Compound **1** was synthesized by condensation of dipyrrylmethane with an equimolar mixture of benzaldehyde and ferrocenecarboxaldehyde. Pure **1** was separated from crude mixtures by column chromatography, and 5,15-diphenyl-2,8,12,18-tetraethyl-3,7,13,17-tetramethylporphyrin (**2**) was also obtained as a side-product in 28% yield but 5,15-diferrocenyl-2,8,12,18-tetraethyl-3,7,13,17-tetramethylporphyrin was not formed, because of steric demand.

The X-ray study of **1** shows that an asymmetric cell consists of one toluene solvent molecule and two ferrocenylporphyrins to form a dimer owing to a π–π interaction between the porphyrin planes. As shown in Fig. 1, the linked cyclopentadienyl (Cp) ring of the ferrocene substituent and the porphyrin plane twisted with dihedral angles of 47.1(3) and 49.3(3)°. The unusually small dihedral angles caused by large steric hindrance of β-pyrrolic methyl group imply that there might be a chance for a weak π-overlap between the Cp and the porphyrin rings. Furthermore, large steric hindrance of the β-pyrrolic methyl groups not only prevents the ferrocenyl moiety from rotating around the *meso* carbon but also results in distortion of the porphyrin ring. The C–C distance (1.50 Å) between the Cp and *meso* carbon of porphyrin is not significantly shorter than the pure single bond distance (1.52 Å) found in the 5,15-diferrocenylporphodimethene [12]. However, It should be considered that this bond distance of other ferrocenyl porphyrin complexes characterized by our and other group was in the range of 1.477(5) ~ 1.498(8) Å which are significantly shorter than 1.52(1) Å. [6a,13] The conjugated feature of **1** was further explored by spectroscopic and electrochemical means. Selected bond distances and angles are listed in Table 2.

Table 2
Selected bond distances (Å) and angles (°) of **1**·$0.5C_6H_5Me$

Fe1–C21	2.072(6)	Fe1–C22	2.050(7)
Fe1–C23	2.038(7)	Fe1–C24	2.009(7)
Fe1–C25	2.013(7)	Fe1–C26	2.024(8)
Fe1–C27	2.026(8)	Fe1–C28	2.03(1)
Fe1–C29	2.02(1)	Fe1–C30	2.015(9)
C4–C5	1.383(8)	C5–C6	1.427(8)
C5–C21	1.505(9)	C15–C43	1.503(8)
C14–C15	1.391(8)	C15–C16	1.397(8)
N1–H1	0.948	N3–H3	0.952
C4–C5–C6	122.1(6)	C4–C5–C21	124.1(6)
C6–C5–C21	113.1(5)	C16–C15–C14	124.9(5)
C16–C15–C43	117.8(5)	C14–C15–C43	117.1(5)
Hydrogen bonding parameters			
N2...H1	2.021(5)	N4...H3	1.910(5)
N1...N2	2.692(7)	N3...N4	2.718(7)
N1...N4	3.160(7)	N2...N3	3.123(7)

Table 3
Half-wave potentials of porphyrin **1**, Zn·**1**, MnCl·**1**

Compound	$E_{1/2}$ (V) [a]		
	Ferrocene oxidation	Porphyrin oxidation	
1	0.29	0.61	1.05
Zn·**1**	0.22	0.45	0.83
MnCl·**1**	0.37	0.97 [b]	
Ferrocene	0.37		

[a] Obtained in CH_2Cl_2 solution containing 0.1 mol dm^{-3} TBAP as supporting electrolyte. Solutions were 1×10^{-3} mol dm^{-3} in compound and potentials were determined with reference to a Ag–AgCl electrode with 0.1 V s^{-1} scan rate.

[b] Two-electron process.

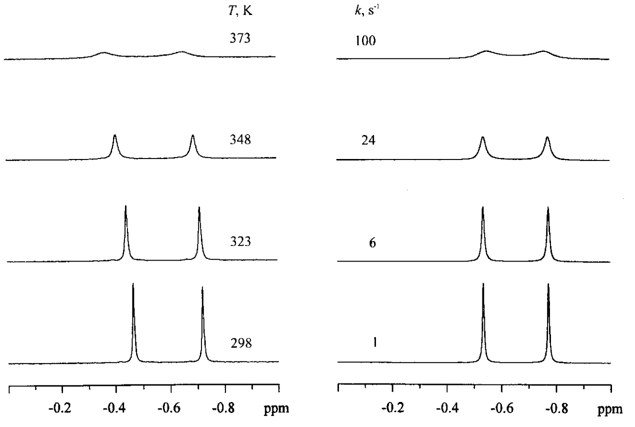

(a) (b)

Fig. 2. Variable temperature ^{1}H NMR spectra for the nitrogen-bonded inner protons of porphyrin **1** in dry toluene-d_8. (a) observed and (b) calculated.

Electrochemical properties of **1** and its metal complexes Zn·**1** and MnCl·**1** in dichloromethane solution are summarized in Table 3. The ferrocenyl groups of compounds **1** and Zn·**1** undergo a reversible one-electron transfer process at 0.29 and 0.22 V, respectively. The values of half-wave oxidation potentials indicate that the ferrocenyl groups in these compounds are more susceptible for the oxidation than the free ferrocene. The easier ferrocenyl oxidation might be considered as a consequence of the great electron releasing ability of the porphyrin ring. In the case of MnCl·**1**, the higher oxidation state of Mn(III) is expected to reduce the electron releasing tendency of the porphyrin ring and thus make the ferrocene oxidation difficult. In fact, the oxidation potential of MnCl·**1** shifts to positive direction. The foregoing electrochemical analyses show that the oxidation of the ferrocene subunit is strongly affected by porphyrin ring as well as the central metal through extended π-conjugation.

^{1}H NMR data further support the strong electronic interaction of the ferrocenyl group with the porphyrin ring. In the case of **1** in chloroform, an electron withdrawing effect of ferrocenyl group through π-conjugation with the porphyrin ring was suggested to account for the large downfield shift of β-pyrrolic methyl protons adjacent to ferrocenyl group (3.35 ppm) compared to those adjacent to phenyl group (2.39 ppm). Furthermore, the chemical shifts for *meso* CH (9.86 ppm) and NH (− 1.06 and − 1.32 ppm) protons of **1** are quite different from the chemical shift for *meso* CH (10.22 ppm) and NH (− 2.41 ppm) protons of **2**. This indicates that the ring current in **1** might be partially reduced due to the ring distortion [14]. Notably, the large downfield shift of NH for **1** compared to **2** can be interpreted by the N–H···N intramolecular hydrogen bonding [15].

The NH tautomerism in porphyrin is an intramolecular proton transfer process coupled with migration of double bonds. The two NH protons of the porphyrin **1** are situated on different chemical environments. Variable temperature ^{1}H NMR spectra of **1** in toluene-d_8 show two distinct singlets of equal intensities and line widths for NH protons as shown in Fig. 2. The chemical shifts are − 0.47 and − 0.72 ppm at 298 K. The presence of ferrocenyl substituent at only C5 position renders the two nitrogen-bonded protons magnetically nonequivalent at room temperature. The coalescence of the two NH peaks was unobserved up to the higher temperature limit of 373 K and only line broadening occurred, indicating that the exchange rate is very slow. This observation can be explained by considering that one kind of intramolecular N–H···N hydrogen bonding is prevailing against the other due to a rectangular

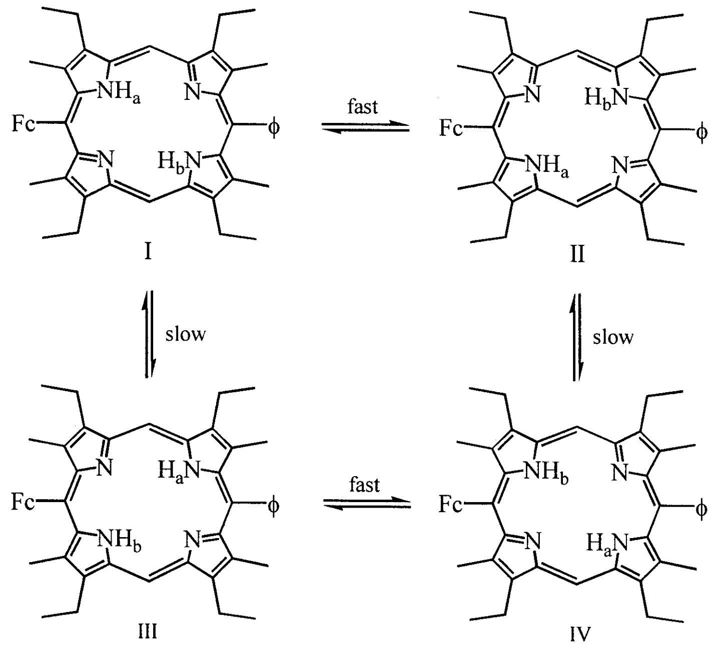

Scheme 1. Schematic representation of NH tautomerism.

elongation of porphyrin core. The X-ray analysis shows that **1** has two sets of short (2.69 and 2.72 Å) and long (3.12 and 3.16 Å) N···N distances and the short N···N distances lie in the known range (2.71 Å) observed for the N–H···N hydrogen bonding units of porphyrin [15]. Thus, the tautomerisations between tautomer I and III as well as between II and IV are not energetically favorable (Scheme 1) [16]. Based on the assumption that exchange is only responsible for the temperature-dependent line broadening, the rate constants for exchange can be determined. From plot of ln (k/T) versus $1/T$ according to Eyring equation [17], a straight line with $\Delta G^{\ddagger} = 51$ kJ mol^{-1} was obtained. This is similar to values reported in the literatures [18]. The exchange rate for NH protons depends on the solution conditions. When anhydrous chloroform is employed as a NMR solvent for **1**, the coalescing of the two NH peaks is not observed up to the higher temperature limit of 328 K. This is similar to the result observed in dry toluene as shown in Fig. 3. However, two NH signals are coalesced below room temperature in chloroform containing trace amount of residual water. It implies that the NH tautomerism of **1** in wet chloroform may be mediated by the trace amount of water in solvent. In dilute solution (0.04 mmol dm^{-3}) of porphyrin, the signal of NH protons is a singlet at 298 K. However, in concentrated solution (0.5 mmol dm^{-3}), the signals of NH protons split into two peaks because the rate of exchange becomes slower. Such result suggests that the rate of dynamic exchange of NH protons is accelerated in proportion to the water concentration of solution.

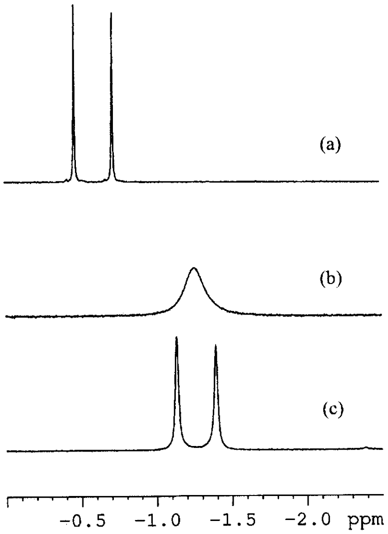

Fig. 3. ^{1}H NMR spectra of **1** in various solvent conditions at 298 K. (a) H_2**1**·0.5C_6H_5Me in anhydrous toluene-d_8, (b) H_2**1** in wet chloroform-*d*, and (c) H_2**1** in anhydrous chloroform-*d*.

4. Supplementary material

Crystallographic data for the structural analysis have been deposited with the Cambridge Crystallographic Data Centre, CCDC No. 140998. Copies of this information may be obtained free of charge from The Director, CCDC, 12 Union Road, Cambridge, CB2 1EZ, UK (fax: +44-1223-336033; e-mail: deposit@ccdc.cam.ac.uk or www: http://www.ccdc.cam.ac.uk).

Acknowledgements

This work was supported by the Korea Science and Engineering Foundation (981-0308-135-2).

References

[1] J. Jortner, M. Ratner (Eds.), Molecular Electronics, IUPAC, Blackwell, Oxford, 1997.

[2] (a) M.A. Fox, Acc. Chem. Res. 32 (1999) 201. (b) I. Willner, B. Willner, J. Mater. Chem. 8 (1998) 2543.

[3] (a) H. Kurreck, M. Huber, Angew. Chem., Int. Ed. Engl. 34 (1995) 849. (b) M.R. Wasielewski, Chem. Rev. 92 (1992) 435.

[4] (a) S.I. Yang, J. Seth, T. Balasubramanian, D. Kim, J.S. Lindsey, D. Holten, D.F. Bocian, J. Am. Chem. Soc. 121 (1999) 4008. (b) J.P. Strachan, S. Gentemann, J. Seth, W.A. Kalsbeck, J.S. Lindsey, D. Holten, D.F. Bocian, Inorg. Chem. 37 (1998) 1191. (c) S.I. Yang, R.K. Lammi, J. Seth, J.A. Riggs, T. Arai, D. Kim, D.F. Bocian, D. Holten, J.S. Lindsey, J. Phys. Chem., Part B 102 (1998) 9426.

[5] (a) T. Yamamoto, T. Morikita, T. Maruyama, K. Kubota, M. Katada, Macromolecules 30 (1997) 5390. (b) B. Bildstein, M. Schweige, H. Kopacka, K.-H. Ongania, K. Wurst, Organometallics 17 (1998) 2414. (c) J.T. Lin, J.J. Wu, C.-S. Li, Y.S. Wen, K.-J. Lin, Organometallics 15 (1996) 5028. (d) D. Posselt, W. Badur, M. Steiner, M. Baumgarten, Synthetic Metals 55 (1993) 3299. (e) M.J. Cohn, M.D. Timken, D.N.J. Hendrickson, Am. Chem. Soc. 106 (1984) 6683.

[6] (a) P.D.W. Boyd, A.K. Burrell, W.M. Campbell, P.A. Cocks, K.C. Gordon, G.B. Jamneson, D.L. Officer, Z. Zhao, Chem. Commun. (1999) 637. (b) A.K. Burrell, W.M. Campbell, D.L. Officer, Tetrahedron Lett. 38 (1997) 1249. (c) N.L. Loim, N.V. Abromova, V.I. Sokolov, Mendeleev Commun. (1996) 46. (d) R.G. Wollmann, D.N. Hendrickson, Inorg. Chem. 16 (1977) 3079.

[7] E.S. Schmidt, T.S. Calderwood, T.C. Bruice, Inorg. Chem. 25 (1986) 3718.

[8] D.D. Perrin, W.L.F. Armarego, Purification of Laboratory Chemicals, Pergamon Press, NewYork, 1988.

[9] D.T. Sawyer, A. Sobkowiak, J.L. Roberts Jr., Electrochemistry for Chemists, Wiley, New York, 1995.

[10] (a) R. Young, C.K. Chang, J. Am. Chem. Soc. 107 (1985) 898. (b) G.M. Sanders, M. van Dijk, A. van Veldhuizen, H. van der Plas, U. Hofstra, T.J. Schaafsma, J. Org. Chem. 53 (1988) 5272.

[11] A. Osuka, T. Nagata, F. Kobayashi, K. Maruyama, J. Heterocycl. Chem. 27 (1990) 1657.

[12] S.W. Rhee, Y.H. Na, Y. Do, J. Kim, Inorg. Chim. Acta (in press).

[13] S.W. Rhee, Y.H. Na, Y. Do, J. Kim (unpublished results).

[14] J.A. Shelnutt, X.-Z. Song, J.-G. Ma, S.-L. Jia, W. Jentzen, C.J. Medforth, Chem. Soc. Rev. 27 (1998) 31, and references therein.

[15] M.S. Somma, C.J. Medforth, N.Y. Nelson, M.M. Olmstead, R.G. Khoury, K.M. Smith, Chem. Commun. (1999) 1221.

[16] M. Asakawa, H. Toi, Y. Aoyama, H. Ogoshi, J. Org. Chem. 57 (1992) 5796.

[17] (a) H. Eyring, Chem. Rev. 17 (1935) 65. (b) S. Glasstone, K.J. Laidler, H. Eyring, The Theory of Rate Processes, McGraw-Hill, New York, 1941. (c) J. Sandström, Dynamic NMR Spectroscopy, Academic Press, New York, 1982.

[18] (a) R.J. Abraham, G.E. Hawkes, K.M. Smith, Tetrahedron Lett. 16 (1974) 1483. (b) K.M. Kadish, K.M. Smith, R. Guilard, The Porphyrin Handbook; Academic Press, Burlington, MA, 1999.